IEEE/CSC & ESAS European Superconductivity News Forum (ESNF), No. 15, January 2011
The published version of this manuscript appeared in *IEEE Transactions on Applied Superconductivity* **21**, Issue 3, 2588 - 2592 (2011)

A Model to Study Plastic Deformation in Nb_3Sn Wires

E. Barzi, M. Bossert, G. Gallo

***Abstract*— An important part of superconducting accelerator magnet work is the conductor. To produce magnetic fields larger than 10 T, brittle A15 conductors are typically used. The original round wire, in the form of a composite of Copper (Cu), Niobium (Nb) and Tin (Sn), is assembled into a so-called Rutherford-type cable, which is used to wind the magnet. The magnet is then subjected to a high temperature heat treatment to produce the chemical reactions that make the material superconducting. At this stage the superconductor is brittle and its superconducting properties sensitive to strain. This work is based on the development of a 2D finite element model, which simulates the mechanical behavior of Nb-Sn composite wires under deformation before heat treatment. First the composite was modeled in detail and its behavior analyzed under flat rolling using Finite Element Analysis (FEM). To identify a critical criterion, the strain results of the model were compared with those measured experimentally on cross sections of the deformed composite. Then the model was applied to a number of different wire architectures.**

***Index Terms*—Nb_3Sn wires, Restacked-Rod Process, Finite Element Model analysis, Principal strain, Plastic work.**

I. INTRODUCTION

WITH progress and the continuous interest in A15 materials for superconducting magnets, a number of finite element models of deformed wires and cables were developed both in the High Energy Physics [1-3] and the Fusion [4, 5] communities. These models are used to predict strand deformation effects and, in some cases, to produce systematic studies as an aid in the design of the wire architecture. In [1, 2] a plastic model was used to analyze a large number of internal Sn strand designs at deformations between 24% and 48%. The critical parameter chosen for such model was the thickness of the Nb barrier surrounding the hexagonal Nb-Sn subelements. The comparison with the data was qualitative only, and because the model extended beyond the failure limit of the composite, pictures of strand cross sections showed a good match with the model predictions only at the lowest deformation levels. However, the model showed a number of very interesting effects and was used for relative comparisons between the various wire architectures. In [3], the model was elastic, with plastic behavior being represented through contact elements, the deformation range was between 14% and 36%, and the critical parameters used were the maximum horizontal, vertical and rotational strains in the cross section plane.

In the present work, to produce an as realistic model as possible of the effects of deforming Restacked-Rod Processed (RRP) wires manufactured by Oxford Superconducting Technology [6, 7], an accurate analysis was performed of the failure mechanisms in the Nb-Sn composite. This allowed determining also the applicable parameters range for the model. For the choice of a critical parameter, a sensitivity analysis to the material properties was performed for stress and strain. Eventually a principal strain was defined and chosen as critical parameter. Finally, we attempted to identify a critical criterion, i.e. max. limit on principal strain, for designers to use. To this end, physics accuracy was first evaluated by systematic comparisons between experimental data and model. Subelement deformations were measured on wire cross sections and compared with those obtained from the model's displacements.

In the following, the failure mode analysis from the data, the model, the sensitivity analysis, the principal strain definition, and the identification of a critical criterion are described. As an example of the model applications, results are shown on the effect of Cu spacing between the Nb-Sn subelements.

II. FAILURE MODE IN RRP Nb_3Sn

In RRP Nb-Sn composite wires, it appears that the outer walls of the Nb-Sn bundles actually merge together only after the Cu channels between the bundles become thin enough. This can be seen in the sequence of pictures in Fig. 1, showing the effect of increasing deformation in an RRP wire with 108 Nb-Sn subelements. Deformation was applied by a flat roller system to round wires before any reaction. Motorized rollers are used to flatten the strand vertically, and the wire is free to expand laterally (see also Fig. 7). The wire diameter was reduced by amounts of 10% to 30% in incremental steps of 4%. At 18% deformation (Fig. 1, top left), the Cu gets thinner in the innermost channels. The Nb-Sn bundles start touching as soon as the Cu channel thickness goes to zero, i.e. breaks, which occurs at 22% deformation (Fig. 1, top right). At 26% deformation (Fig. 1, bottom left) the Nb starts breaking in the innermost bundles and merging radially outward. Eventually, at 30% deformation (Fig. 1, bottom right), the merging has encompassed the whole thickness of the superconducting area.

A study on 214 strand samples of RRP wire with 108 Nb-

Manuscript received August 3, 2010.
This work was supported by the U.S. Department of Energy.
All authors are with the Fermi National Accelerator Laboratory (Fermilab), P.O. Box 500, Batavia, IL 60510 USA (phone: 630-840-3446; fax: 630-840-3369; e-mail: barzi@fnal.gov).

Sn subelements deformed between 10% and 30% confirmed that breakage in this wire starts at 26% deformation. Fig. 2 shows the number of damaged subelements in each circular row of the superconducting hexagonal area, normalized to the number of cross sections (CS) analyzed, as function of wire deformation.

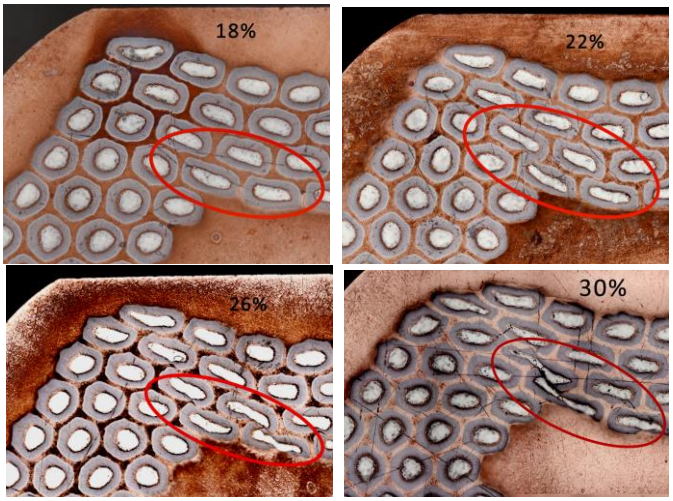

Fig. 1. Sequence of pictures showing the effect of increasing deformation in Restacked-Rod-Processed (RRP) Nb-Sn composite wires.

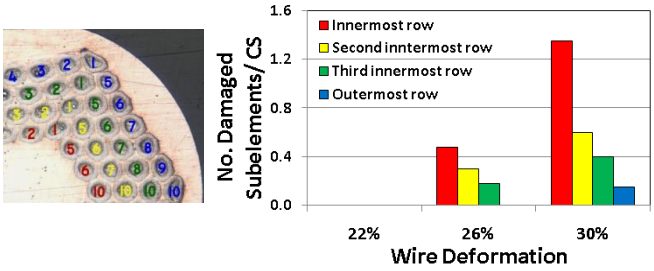

Fig. 2. Number of damaged subelements in each circular row of the superconducting hexagonal area of an RRP wire with 108 Nb-Sn subelements, normalized to the number of cross sections (CS) analyzed, as function of wire deformation.

III. Model Description and Results

The 2D ANSYS model [8] included an environment pre-processor and an environment solution. The former was used to describe strand geometry, elastic and plastic material properties by means of bi-linear stress-strain curves [9, 10], and constraints. The hypotheses used were of plain strain (i.e. infinite wire length with zero axial strain) and isotropic behavior. ANSYS element plane-82 was used. The mesh (element size) was optimized in order to provide much finer information in the Cu channels between bundles. The environment solution was a non-linear analysis (algorithm used Newton-Raphson equations). The load was provided as displacement of a rigid contact element (Target-169) applied gradually on the external surface of the wire. A flexible contact element was used on the wire surface (Contact-172). The number of load steps and sub-steps was optimized for accuracy.

Two different load orientations were considered, as shown in Fig. 3. At left, the wire displacement is applied parallel to the side of the hexagonal superconducting area. At right, the displacement is imparted on the edge. When a wire deformation of 26% was used in both load cases for a wire with 108 Nb-Sn subelements, the former load configuration produced a maximum plastic work per unit volume in the cross section (Fig. 4, left) that was 30% larger than that obtained in the latter load configuration (Fig. 4, right). The former load configuration was therefore chosen in all subsequent simulations.

Figs. 5 and 6 (left) show the three strain component distribution in the cross section of a wire with 108 Nb-Sn subelements reduced by 26% in size. It was interesting to notice that none of the strain components alone would predict the failure locations observed in RRP wires deformed to 26% deformation (Figs. 1, 2 and 7). Instead, it was found that both the plastic work density and the Von Mises strain, shown in Figs. 4 and 6 (right), were good pointers to the wire critical locations.

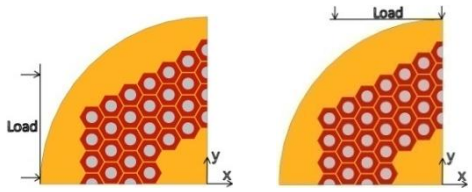

Fig. 3. Load orientations that were considered.

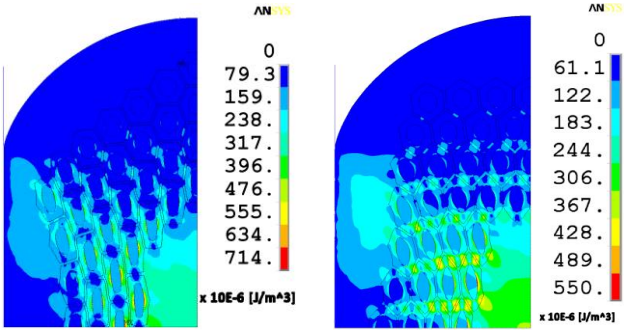

Fig. 4. Plastic work per unit volume at 26% wire deformation in the two load configurations.

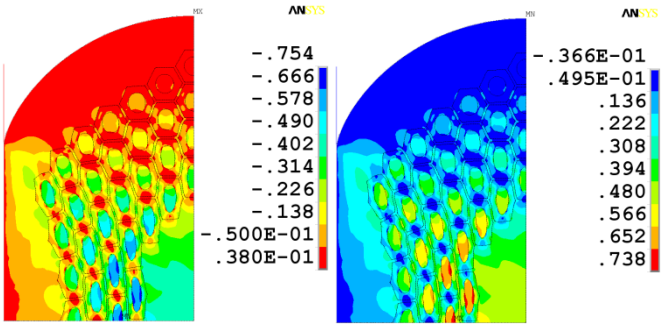

Fig. 5. Strain_x (left) and Strain_y (right) at 26% wire deformation.

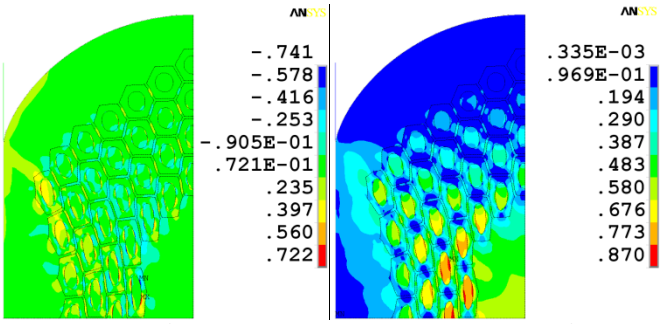

Fig. 6. Strain_xy (left) and Von Mises strain (right) at 26% wire deformation.

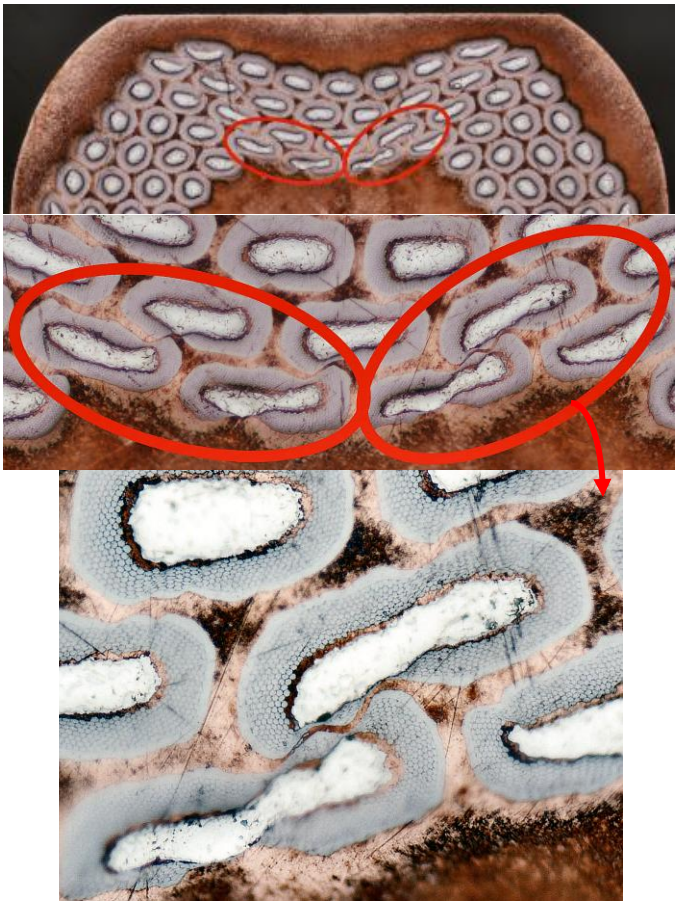

Fig. 7. RRP wire with 108 Nb-Sn subelements flat rolled at 26% deformation showing failure locations.

A. *Choice of critical parameter*

The main criterion used in the choice of a representative, or critical, parameter for this model was its sensitivity to the inputs parameters, and particularly to the plastic material properties. As is well known, whereas the Young modulus E is usually well established in the elastic regime, for bi-linear stress-strain curves, as in Fig. 8, there may be large uncertainties on the exact values of the Tangent modulus and sometimes also of the Yield Tensile Strength (H and YS in Fig. 8). Using a wire deformation of 18%, the model was run 18 times by separately varying Nb, Sn and Cu Tangent moduli (for each, H=E/100, E/50 and E/10 were used), and their Yield Tensile Strengths (for each, three YS values were chosen ranging from hot worked to cold worked material values). The model parameters used in this sensitivity analysis were strain_y and stress_y in the four innermost Cu channels A to D in Fig. 9. The model was most sensitive to the Cu Tangent modulus. However, whereas the average stress_y in the Cu channels increased by 680% when the Cu tangent module was increased tenfold, the average strain_y decreased by only 50% The source of maximum variation when analyzing the effect of YS was the Nb, whose maximum increase in YS produced variations of 40% of both stress_y and strain_y in the Cu channels. These combined results indicated that strain would be a more appropriate critical parameter than stress.

However good as an indicator of critical areas the Von Mises strain may be, it cannot be used in plastic problems. Therefore, a principal tensor strain was defined in the Cu channels as that represented by a pure shear Mohr circle (see Fig. 10). The principal traction strain was found to be the largest in the Cu channels between the innermost row of subelements and the next (see map in Fig. 11), with the maximum value associated to either the first or the second diagonal lines in the map of Fig. 11. Fig. 12 shows such principal strain in the innermost channels as function of their angular position, clockwise, starting from the first diagonal line, for a wire with 108 Nb-Sn subelements deformed by 26% in size. The principal strain values decreased radially outward along each diagonal line. This can also be seen in Fig. 18.

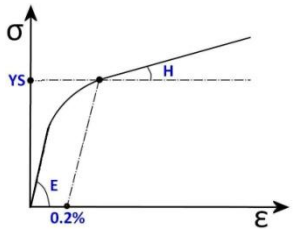

Fig. 8. Bi-linear stress-strain curve.

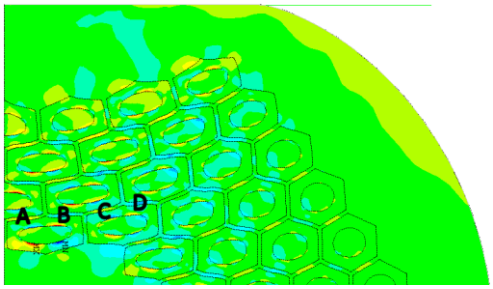

Fig. 9. Cu channels A to D used in model sensitivity analysis.

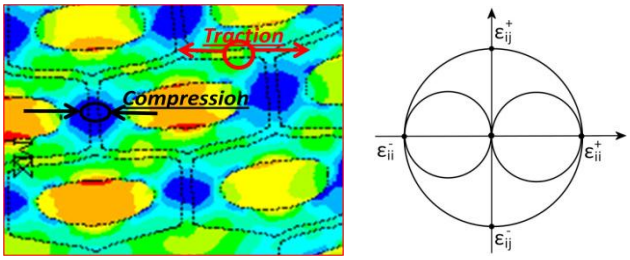

Fig. 10. Close-up of Von Mises strain distribution at 18% deformation (left). A principal tensor strain was defined in the Cu channels as that represented by a pure shear Mohr circle (right).

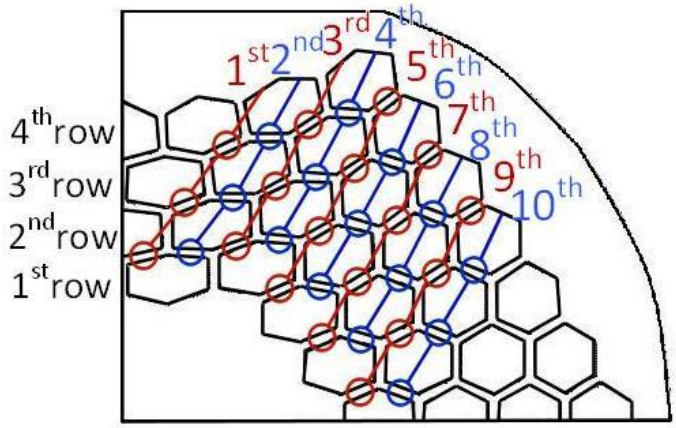

Fig. 11. Location map used in deformed wire.

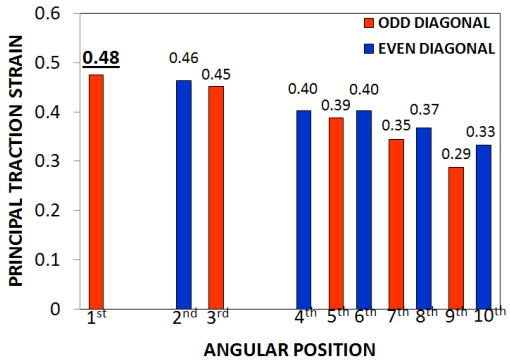

Fig. 12. Principal traction strain in the Cu channels between the 1st innermost row of subelements and the next outward for a wire with 108 Nb-Sn subelements at 26% deformation.

B. *Effect of Cu Spacing between Nb-Sn Bundles*

The effect of Cu spacing between subelements in RRP wires has been studied for a strand with 108 Nb-Sn bundles at 18% deformation. The model has been run for Cu thicknesses from 4.8 µm, corresponding to a spacing factor of 1, to 16.8 µm, corresponding to a spacing factor of 3.5, in incremental steps of 0.5 for the spacing factor. Fig. 13 shows the principal traction strain in the Cu along the 2nd (Fig. 11) critical diagonal as function of radial position. Tripling the Cu thickness decreases the maximum principal traction strain by ~10%.

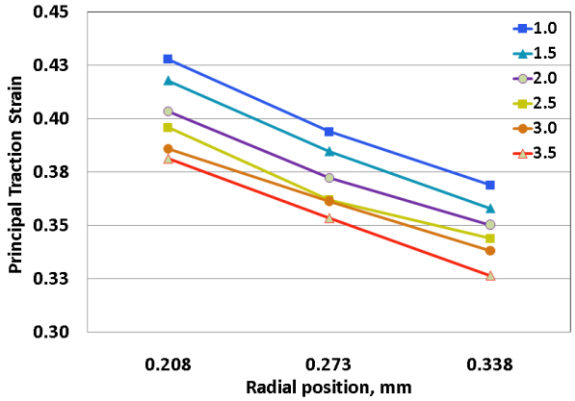

Fig. 13. Maximum principal traction strain in the Cu along 2nd critical diagonal in Fig. 11 as function of radial position.

IV. Identification of Critical Criterion

For the identification of a representative and usable critical criterion, i.e. max. limit on principal strain, physics accuracy of the model had to be evaluated. This was done by systematic comparisons between experimental data and model. Subelement deformations were measured along the short and long sizes of the hexagonal bundles on wire cross sections and compared with those obtained from the model's displacements (see Fig. 14). Fig. 15 shows the comparison between data and model of the average deformation of the subelements along the critical diagonal line (2nd diagonal line in Fig. 11) as function of the wire's reduced diameter. Fig. 16 compares data and model results of the average deformations of the subelements in the innermost row, as function of the wire's reduced diameter.

Because of the very good correlation with the data in the two most critical areas of the conductor, i.e. the critical diagonal line and the innermost circle of bundles, for loads approaching the critical load of 26%, the value of the maximum principal traction strain obtained in Fig. 12 could be used as a critical criterion for RRP wires. For the Nb-Sn bundles not to merge and start breaking, the principal traction strain in the Cu should not exceed 0.48 ± 0.10. The 0.10 strain uncertainty was the maximum discrepancy between data and model obtained on the deformation values of the most deformed subelement in the wire cross section.

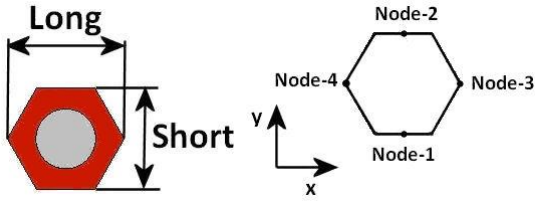

Fig. 14. Definition of subelement sizes (left), and subelement nodes used in calculating model's displacements (right).

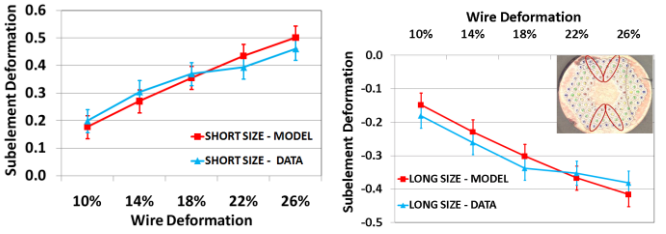

Fig. 15. Comparison between data and model of the average deformations, along the short (left) and long (right) sizes, of the subelements on the critical diagonal line, as function of wire deformation.

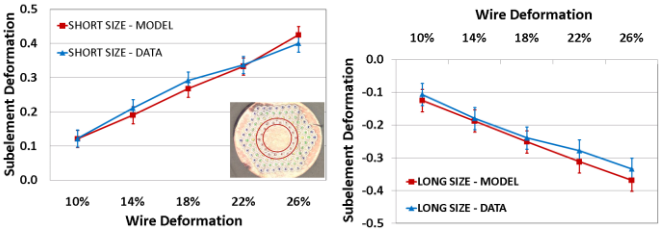

Fig. 16. Comparison between data and model of the average deformations, along the short (left) and long (right) sizes, of the subelements in the innermost row, as function of wire deformation.

A. *Test of Critical Criterion Using Different Architectures*

To test the soundness of the critical criterion range identified above, RRP wires with other architectures were modeled and experimentally analyzed. The RRP wire with 108 Nb-Sn subelements (Fig. 17, left) was compared to a similar architecture without corners with 102 Nb-Sn bundles (Fig. 17, center) and to an architecture also without corners but with an additional inner row of Nb-Sn subelements and a total of 114 bundles (Fig. 17, right). The three designs were modeled at 26% wire deformation and the principal traction strain in the Cu along the 2nd diagonal was plotted in Fig. 18 as a function of radial position. The plastic work per volume follows the same behavior. Because the principal strain increases radially when moving toward the center of the strand, the wire with the additional inner row sees the largest strain. The model was then run for the three designs also at 18%, 22% and 30%

deformation levels. Results are shown in Fig. 19, which shows the maximum principal traction strain found in the cross section for all designs as a function of wire deformation. The maximum principal traction strain in the cross section increases faster with deformation in the 114 subelement design than in either the 102 or the 108 design.

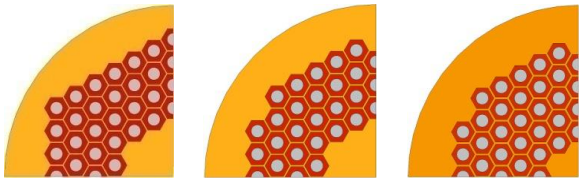

Fig. 17. RRP 108/127 (left), RRP 102/127 (center) and RRP 114/127 (right).

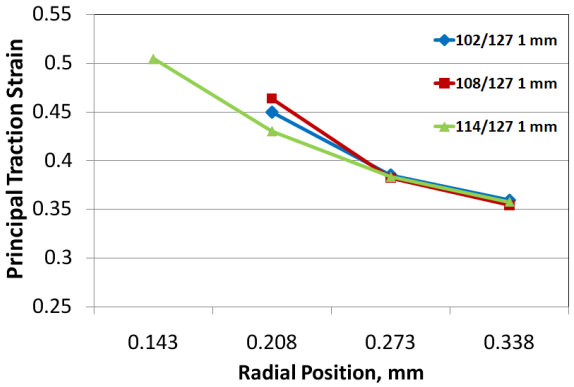

Fig. 18. Principal traction strain in the Cu along the 2nd diagonal at 26% deformation as a function of radial position for designs with 102, 108 and 114 Nb-Sn subelements.

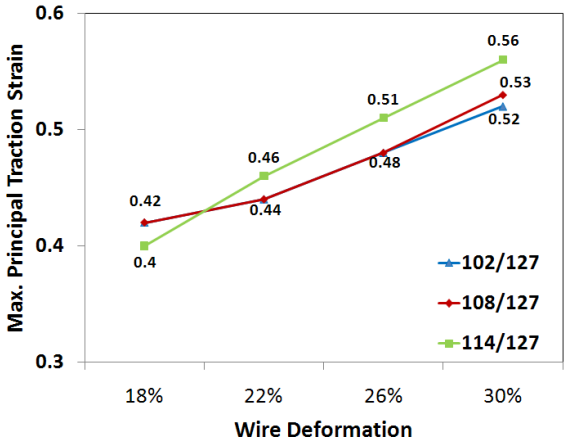

Fig. 19. Maximum principal traction strain in the wire cross section for designs with 102, 108 and 114 Nb-Sn subelements as function of wire deformation.

The data were consistent in that an experimental study on 454 deformed samples with 102, 108 and 114 subelements showed that damage to the Nb-Sn bundles in the 114 subelements design starts at only 22% deformation (at which the calculated max. principal strain in the Cu is 0.46), and a larger fraction of bundles gets damaged once such level is exceeded. Instead, the designs with 102 and 108 subelements behave very similarly over the analyzed deformation range. This is shown in Fig. 20, which plots the number of damaged subelements per cross section found experimentally at each level of deformation for the three designs.

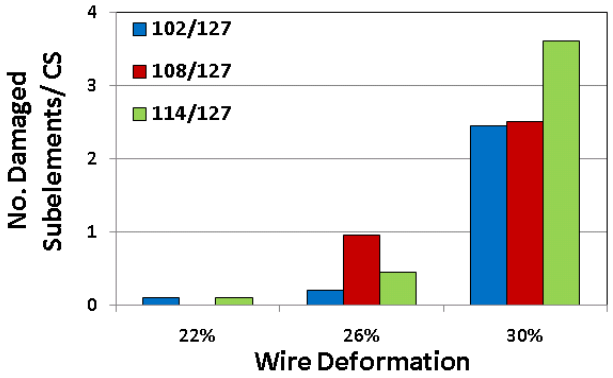

Fig. 20. Number of damaged subelements per cross section found experimentally as function of wire deformation for designs with 102, 108 and 114 Nb-Sn subelements.

V. Conclusions

In RRP Nb-Sn composite wires, the outer walls of the Nb-Sn bundles merge together only after the Cu channels between the bundles become thin enough. Therefore, in the model herein proposed, a principal tensor strain was defined in the Cu channels. Because the principal strain increases radially when moving toward the center of the strand, wires with additional inner rows see the largest strains. It was also found that increasing the Cu thickness between Nb-Sn bundles decreases the maximum principal strain.

The very good correlation between model and data also allowed identifying a critical criterion for RRP wires. For the Nb-Sn bundles not to merge and start breaking, the principal traction strain in the Cu should not exceed 0.48 ± 0.10.

Acknowledgment

The authors wish to thank Prof. Marco Beghini and Dr. Ciro Santus for their insights and continuous collaboration.

References

[1] S. Farinon et al., "Finite Element Model to Study the Deformations of Nb_3Sn Wires for the Next European Dipole (NED)", IEEE Transaction Appl. Sup., V. 17, No. 2, pp. 1136-1139 (2007).

[2] S. Farinon, T. Boutboul, A. Devred, D. Leroy and L. Oberli, "Nb_3Sn Wire Layout Optimization to Reduce Cabling Degradation", IEEE Transaction Appl. Sup., V. 18, No. 2, pp. 984-988 (2008).

[3] M. Alsharoa'a et al., "Optimization of Brittle Superconducting Nb_3Sn Strand Designs", IEEE Transaction Appl. Sup., V. 18, No. 2, pp. 1496-1499 (2008).

[4] H. Bajas, D. Durville, D. Ciazynski, A. Devred, "Numerical Simulation of the Mechanical Behavior of ITER Cable-In Conduit Conductors", IEEE Transaction Appl. Sup., V. 20, No. 3, pp. 1467-1470 (2010).

[5] D. P. Boso, M. Lefik, B. A. Schrefler, "A multilevel homogenized model for superconducting strand thermomechanics", CRYOGENICS V. 45, No. 4, pp. 259-271 (2005).

[6] E. Barzi et al., "Performance of Nb_3Sn RRP Strands and Cables Based on a 108/127 Stack Design", IEEE Trans. Appl. Sup., V. 17, No. 2, p. 2718 (2007).

[7] M. B. Field, J. A. Parrell, Y. Zhang, M. Meinesz, and S. Hong, "Internal tin Nb_3Sn conductors for particle accelerators and fusion applications", Adv. Cryo. Engr., V. 54, pp. 237-243 (2008).

[8] ANSYS, Inc., Southpointe, 275 Technology Drive. Canonsburg, PA, 15137, U.S.A. Available online: http://www.ansys.com.

[9] *Atlas of stress-strain curves*, 2nd Ed. The materials information society-ASM International, Materials Park, OH.

[10] MatWeb. Material Property Data. Available online: http://www.matweb.com.